Letters

An Enhanced DC Preexcitation With Effective Flux-Linkage Control for the High-Power Induction Motor Drive System

Sideng Hu, Zhengming Zhao, Hua Bai, and Liqiang Yuan

***Abstract*—This paper proposed an enhanced dc preexcitation for a variable-voltage variable-frequency-controlled induction motor drive system. Voltage vectors were adjusted according to the reactive component of the motor current, which promptly established the effective value of the motor flux linkage at the preexcitation stage and restrained its trajectory strictly as a round circle all through the starting process. The enhanced dc preexcitation control led to more negligible flux-linkage distortion, less torque vibration, and significantly smaller inrush current. Experiments on a 380-VAC/315-kW adjustable speed drive system validated the effectiveness of the proposed method.**

***Index Terms*—Adjustable speed drive (ASD) system, dc preexcitation, induction motor (IM), startup, variable-voltage variable frequency (VVVF).**

I. Introduction

In motor drive systems, the startup control is always a critical issue due to the inrush current in the starting process, which tends to damage the motor insulation and endanger the semiconductor devices [1]–[4]. It is highly related to the absence of the effective flux linkage. Vector controls, e.g., the direct torque control (DTC) and field-oriented control (FOC), have been validated capable of delivering the targeted torque and depressing the startup current through processing the accurate flux-linkage observation and control. However, they suffer from the nonlinearity of power devices and the complication of the parameter identification. Both FOC and DTC face the challenges of the inaccurate flux-linkage observation, which is of particular importance for the sensorless vector control at low-speed operation [5], [6].

One feasible solution is to adopt the variable-voltage variable-frequency (VVVF) control in the starting process and smoothly switch to the sensorless vector control in the high-speed region [7]–[9]. In the previous study [10]–[12], a dc preexcitation control in a three-level VVVF-controlled induction motor (IM) drive system was proposed, which establishes the initial back electromotive force (EMF) before the motor gets started. Therefore, it effectively depressed the inrush current and increased the starting torque. However, its effect will be discounted by the absence of flux-linkage control in the whole starting process. This will lead to the flux-linkage distortion, thereby, the overcurrent and insufficient torque.

As an extension of the previous study on the dc preexcitation [10], this paper will analyze its disadvantages, enhance the dc preexcitation with one simple and effective flux-linkage controller, and validate its effectiveness through simulations and experiments in a two-level three-phase 380-VAC/315-kW motor drive system. Different startup strategies will also be detailed through experiments.

Manuscript received October 17, 2010; revised January 18, 2011; accepted March 6, 2011. Date of current version September 16, 2011. This work was supported by the key program of the National Natural Science Foundation of China under Grant 50737002 and Grant 50707015. Recommended for publication by Associate Editor J. Biela.

S. D. Hu, Z. M. Zhao, and L.Q. Yuan are with the Department of Electrical Engineering, Tsinghua University, Beijing 100084, China (e-mail: hsd06@mails.tsinghua.edu.cn; zhaozm@mail.tsinghua.edu.cn; ylq@tsinghua.edu.cn).

H. Bai is with the Department of Electrical and Computer Engineering, Kettering University, Flint, MI 48504 USA (e-mail: hbai@kettering.edu).

Digital Object Identifier 10.1109/TPEL.2011.2131680

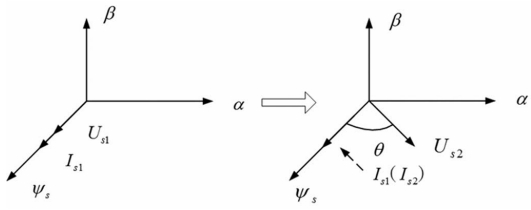

Fig. 1. Vector scheme in the motor start moment: (a) before startup and (b) at the startup moment, I_{s1} and I_{s2} could be viewed as equal.

II. Principles of the DC Preexcitation and its Demerits

DC preexcitation establishes the flux linkage of the IM through imposing a dc current on the motor before it starts up. The stator flux linkage can be expressed as follows:

$$\psi_s = L_s \cdot I_s + L_m \cdot I_r \tag{1}$$

where I_s is the stator current, I_r is rotor current, L_s is the stator leakage inductance, and L_m will be the excitation inductance. In the dc preexcitation, I_r is close to zero. In this case, stator flux linkage can be simplified as follows:

$$\psi_s = L_s \cdot I_s. \tag{2}$$

Fig. 1 shows the voltage vectors at the moment when the dc preexcitation process is switched to the starting process. I_{s1} is the preexcitation current and I_{s2} is the current at the startup moment. As mentioned in [10], I_{s1} and I_{s2} could be viewed as equal at this moment, and the slope of the flux linkage is

$$\frac{d}{dt}\psi_s = \frac{\psi_s(t_s + \Delta t) - \psi_s(t_s)}{\Delta t} = U_{s2} - I_{s1} * R_s \tag{3}$$

where U_{s2} is stator voltage vector in startup process, and R_s is the stator resistance. By cross multiplying I_{s2} at both sides of equation (3),we get

$$\frac{\psi_s(t_s+\Delta t)\otimes I_{s2}-\psi_s(t_s)\otimes I_{s2}}{\Delta t}=U_{s2}\otimes I_{s2}. \quad (4)$$

Since the electromagnetic torque is

$$T_e=p_n(\psi_s\otimes i_s) \quad (5)$$

therefore

$$\left|\frac{dTe}{dt}\right|\approx p_n\left|U_{s2}\otimes I_{s2}\right| \quad (6)$$

where p_n is the pole number in the motor.

Equation (6) is the essence of the previously proposed dc preexcitation, which implies that at the starting moment, a voltage vector U_{s2} perpendicular to the excitation current vector I_{s1} will maximize the torque. Also, the established flux linkage will induce back EMF to effectively restrain the inrush current.

However, (6) can only hold voltage vector perpendicular to excitation current for the first several switching periods during the starting process. When the motor begins rotating, the angle between the voltage vector and the excitation current I_{s1}cannot be guaranteed as direct angle. Therefore, (6) is no longer satisfied, which degrades the effect of the dc preexcitation. This also leads to atrocious amount of effort to get the optimal preexcitation current value, direction, and time, as shown in [10].

Equation (5) can be written as follows:

$$\frac{dTe}{dt}=p_n\left(\frac{d\psi_s}{dt}\otimes I_{s2}+\psi_s\otimes\frac{dI_{s2}}{dt}\right). \quad (7)$$

Since $d\psi_s/dt=U_s-I_sR_s$, (7) could be derived as follows:

$$\frac{dTe}{dt}=p_n\left((U_{s2}-I_{s2}\cdot R_S)\otimes I_{s2}+\psi_s\otimes\frac{dI_{s2}}{dt}\right). \quad (8)$$

In the *d–q* coordinate axis, (8) could be expressed as follows:

$$\frac{dT_e}{dt}=p_n\left(U_s\otimes(I_{sd}+jI_{sq})+\psi_s\otimes\frac{d(I_{sd}+jI_{sq})}{dt}\right). \quad (9)$$

Note here that I_{sd} is the current mapped along the U_s, and I_{sq} is kept vertical to U_s, which is totally different from the traditional *d–q* transformation in FOC. A constant I_{sq} will result in $dI_{sq}/dt=0$. Therefore,

$$\frac{dT_e}{dt}=p_n\left(U_sI_{sq}+\psi_s\otimes\frac{dI_{sd}}{dt}\right). \quad (10)$$

Moreover, digitizing (10) leads to

$$\Delta T=p_n(U_sI_{sq}\Delta t+\Psi_s\otimes\Delta I_{sd}). \quad (11)$$

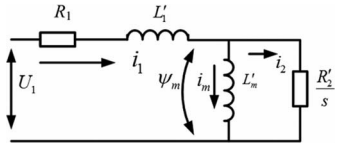

Fig. 2. Equivalent circuit diagram for IM.

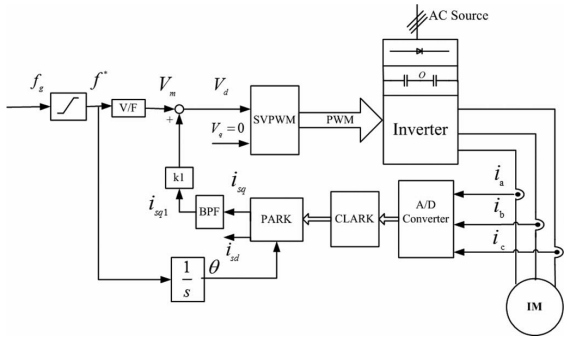

Fig. 3. Diagram of the proposed method.

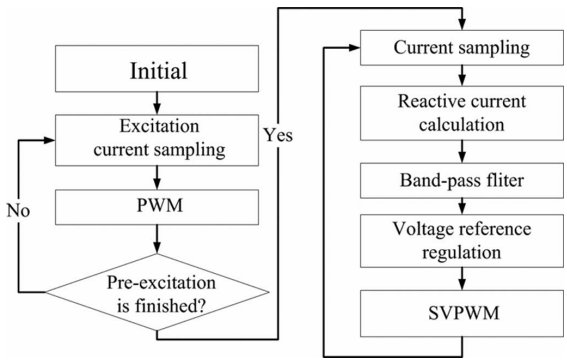

Fig. 4. Flow chart of the proposed method.

Equation (11) extends the effective area of the dc preexcitation to the whole startup process. Equation (6) is only an exception assuming that $dI_{sd}/dt=0$.

III. Enhanced DC Preexcitation

As it was pointed in Section II, $dI_{sq}/dt=0$ is the precondition of (11). However, different from FOC and DTC, the conventional VVVF control is a typical open-loop control without any current decoupling. Here, we need first derived the expression of i_{sd} and i_{sq} based on the equivalent circuit of an IM, as shown in Fig. 2.

I_{sd} and I_{sq} represent the active and reactive current in Fig. 2, respectively, which are expressed as follows, as shown (12) and (13), at the bottom of next page page.

$$I_{sd}=\frac{\left(R_1R'^2_2+\omega^2L'^2_ms^2R_1+\omega^2L'^2_msR'_2\right)U_1}{\omega^4L'^2_1L'^2_ms^2+\left((R_1s+R'_2)^2L'^2_m+2L'_1R'^2_2L'_m+L'^2_1R'^2_2\right)\omega^2+R_1^2R'^2_2} \quad (12)$$

$$I_{sq}=-\frac{\left(\omega L'_1R'^2_2+R'^2_2\omega L'_m+\omega^3L'^2_ms^2L'_1\right)U_1}{\omega^4L'^2_1L'^2_ms^2+\left((R_1s+R'_2)^2L'^2_m+2L'_1R'^2_2L'_m+L'^2_1R'^2_2\right)\omega^2+R_1^2R'^2_2}. \quad (13)$$